

# Endonasal and Transoral Approaches to the Craniovertebral Junction: A Quantitative Anatomical Study



Francesco Doglietto, Francesco Belotti, Jimmy Qiu, Elena Roca, Ivan Radovanovic, Anne Agur, Walter Kucharczyk, Alberto Schreiber, Andrea Bolzoni Villaret, Piero Nicolai, Fred Gentili<sup>§</sup>, and Marco Maria Fontanella<sup>§</sup>

**Abstract** *Background:* The endoscopic endonasal approach has recently been added to the surgical armamentarium to access the anterior craniovertebral junction (CVJ). Comparative analyses with the transoral approach are scarce. The aim of this study was to provide a quantitative anatomical analysis of both approaches.

*Methods:* In four specimens the endoscopic endonasal approach (before and after sphenoidectomy) and the transoral approach (without and with a soft palate split) were performed. ApproachViewer—part of GTx-UHN (Guided Therapeutics software, developed at University Health Network, Toronto, ON, Canada)—was used to quantify and visualize the working volume, as well as the exposed area, of each surgical approach. Different modalities (crossing and non-crossing) were used to quantify the exposure of the deep surface, providing an indirect quantitative value of the ‘surgical freedom’. The lowest point exposed by the endonasal

approaches was compared with that predicted by preoperative radiological lines. Non-parametric Welch analysis of variance (ANOVA) was used for statistical analyses.

*Results:* The working volume was significantly larger and the distance to the target was shorter with the transoral approaches than with the endonasal approaches. Clival exposure was better with the endonasal approaches than with the non-crossing transoral approach without a soft palate split; areas below C1 were better exposed with the transoral routes. The nasoaxial line best predicted surgical exposure with the endonasal approaches.

*Conclusion:* Endoscopic endonasal and transoral approaches to the anterior CVJ provide optimal exposure of different areas that overlap at the level of C1 when no anatomical anomalies are present. A split of the soft palate is not necessary during the transoral approach if it is combined with an endoscopic endonasal approach.

Author contributed equally with all other contributors. Fred Gentili and Marco Maria Fontanella

F. Doglietto (✉) · F. Belotti · E. Roca · M. M. Fontanella  
Neurosurgery, Department of Medical and Surgical Specialties,  
Radiological Sciences and Public Health, University of Brescia,  
Brescia, Italy  
e-mail: [francesco.doglietto@unibs.it](mailto:francesco.doglietto@unibs.it)

J. Qiu · W. Kucharczyk  
Division of Neuroradiology, Department of Medical Imaging,  
University Health Network, Toronto, ON, Canada

Division of Neuroradiology, Department of Surgery, University  
Health Network, Toronto, ON, Canada

I. Radovanovic · F. Gentili  
Division of Neurosurgery, Toronto Western Hospital, Department  
of Surgery, University Health Network, Toronto, ON, Canada

A. Agur  
Division of Anatomy, Department of Surgery, University of  
Toronto, Toronto, ON, Canada

A. Schreiber · A. B. Villaret · P. Nicolai  
Otorhinolaryngology—Head and Neck Surgery, Department of  
Medical and Surgical Specialties, Radiological Sciences and  
Public Health, University of Brescia, Brescia, Italy

**Keywords** Anatomy · Craniovertebral junction · Endonasal Quantitative · Transoral

## Introduction

Endoscopic endonasal approaches to the anterior craniovertebral area have recently been added to the surgical armamentarium for the treatment of pathologies that involve this anatomically complex region [1–3].

Detailed anatomical descriptions of the endoscopic endonasal approach are available [1, 2, 4], but only a few papers have attempted a comparative analysis of this approach and the transoral approach [5–9]. Limited clinical comparative data are available [10].

The aim of this paper is to systematically analyse the anatomical features of the endonasal and transoral routes to the anterior craniovertebral junction (CVJ), using a recently

developed research method that allows visualization and quantification of the surgical pyramid that defines a surgical approach [11, 12].

## Materials and Methods

### Specimens

Four lightly embalmed specimens underwent computed tomography (CT) scans, using a  $1 \times 1$  frame with contiguous slices, at both 1 and 3 mm. CT was performed using a gantry of  $0^\circ$ , with a scan window diameter of 225 mm and a pixel size of more than  $0.44 \times 0.44$  (University of Toronto Research Ethics Board (REB) approval no. 23,849). The CT scan files were saved in DICOM (Digital Imaging and Communications in Medicine) format.

### Surgical Approaches

Surgery was simulated at the University of Toronto Surgical Skills Centre at Mount Sinai Hospital. Endoscopic dissections were performed using a high-definition head camera with  $0^\circ$  and  $30^\circ$  rod-lens scopes (Karl Storz®, Tuttlingen, Germany). Microsurgical dissections were performed under microscopic visualization at  $\times 4$  to  $\times 18$  magnifications. A Crockard retractor (Codman®, Randolph, MA, USA) was used for the transoral approaches.

The *endoscopic endonasal approach to the anterior CVJ* was performed. Using a  $0^\circ$  rod-lens scope. The inferior turbinate was out-fractured to visualize the choana bilaterally. A rubber band was introduced into the nostril and pulled out of the oral cavity bilaterally, so as to retract the soft palate. A right middle turbinectomy and maxillary antrostomy were performed, and a nasoseptal flap was harvested on the right and positioned in the maxillary sinus. A posterior septectomy was performed, taking special care to drill the septum flush with the posterior portion of the hard palate. A linear incision was performed at the level of the rhinopharynx, down to the prevertebral fascia, and the muscles were dissected subperiosteally, exposing the anterior tubercle of the atlas. Then a wide sphenoidectomy was added to the approach, drilling the sphenoid floor to the clival plexus posteriorly and laterally to both the vidian and hypoglossal nerves.

The *microsurgical transoral approach* was also performed. The mouth opening was checked and, if it was abnormal because of the partial fixation of the specimens, it was normalized using an incision at the level of the masseter insertion into the zygoma. Once self-retaining retractors

were positioned, a rubber catheter was placed through the nose and then sutured to the uvula to retract it out of the field. A midline incision was performed at the level of the oropharynx, elevating a single myomucosal flap from the anterior longitudinal ligament.

The soft palate was then divided at its midline from the junction with the hard palate to the side of the uvula, deviating off the midline to preserve it.

### Quantifications

A dedicated software package called ApproachViewer—part of GTx-UHN (Guided Therapeutics software, developed at University Health Network, Toronto, ON, Canada)—was used for the anatomical quantifications [11, 12].

ApproachViewer allows for real-time evaluation and comparison of surgical approaches, as well as postdissection analyses of collected data. It was developed to visualize, in three dimensions (3D), the surgical approach inside the head in which it was performed, as well as quantifying its anatomical features. The quantitative comparison of approaches was therefore based on their anatomical features, defining them as ‘truncated pyramids’, as described by Andaluz et al. [13]. A truncated pyramid is defined by its superficial surface (or ‘surgical window’), deep surface (or ‘area of exposure’), height (the distance between the previous areas) and pyramid volume (the surgical space that is available for straight instruments) (Fig. 1).

Commercially available navigation hardware was used (Northern Digital Imaging®, Waterloo, ON, Canada) and included a passive rigid body, a passive probe (pointer) with four markers, and the Polaris Vicra® optical tracking system. The Polaris optical camera emits infrared (IR) light and captures IR reflections off sphere markers attached to the pointer, whose geometry allows reproduction of its position and orientation with a multiplanar reconstruction.

DICOM files were uploaded into GTx-UHN and a registration tolerance of  $<2$  mm was accepted. In addition to providing neuronavigation during the dissections, ApproachViewer allows collection of deep and superficial surfaces, using the pointer to track their perimeters, and provides real-time visualization and quantification of the surgical pyramid in axial, coronal and sagittal sections, and as a 3D rendering (Fig. 4) [11, 12]. The quantification procedure was repeated twice for each approach, tracking both ‘non-crossing’ and ‘crossing’ pyramids. A non-crossing pyramid is obtained by keeping the pointer in corresponding positions on both deep and superficial surfaces, thus obtaining the widest obstacle-free working space, defined by a straight instrument. A crossing pyramid is obtained by keeping the pointer in opposite positions on

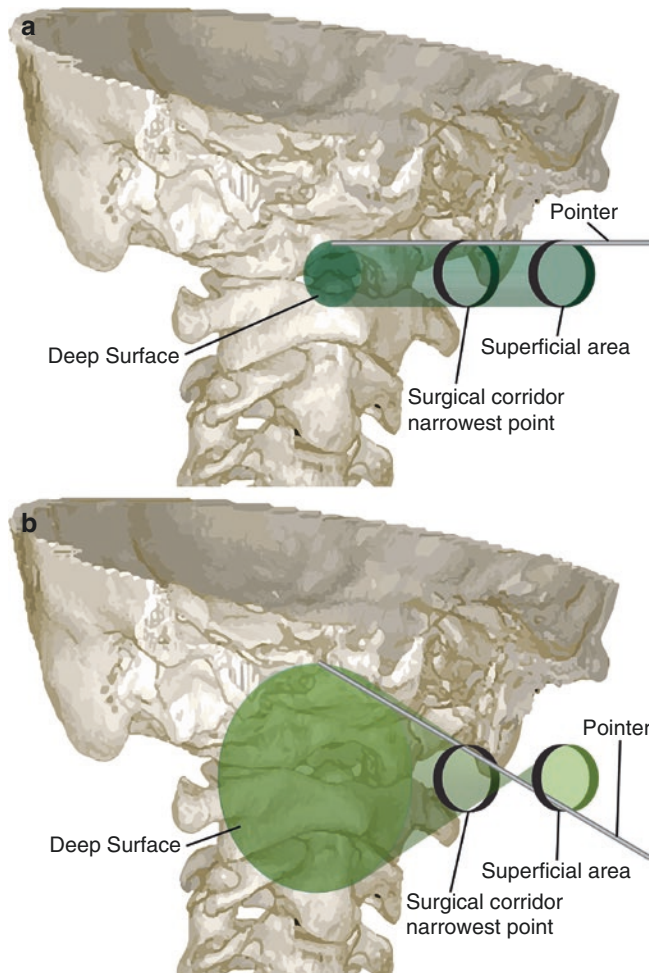


**Fig. 1** Surgical pyramid with ‘non-crossing’ and ‘crossing’ collection modalities. Two different modalities are used to evaluate the working volume of each approach. **(a)** Non-crossing modality: when the pointer is positioned at the level of the deep area, at the anterior craniovertebral junction (CVJ), special care is taken to touch the superficial area at the same level (i.e. the pointer touches the 12 o’clock point on both surfaces). **(b)** Crossing modality: the pointer positioned on the deepest surface is positioned at the opposite level in the superficial area (i.e. the pointer is positioned at 12 o’clock on the deep surface and touches the 6 o’clock point on the superficial area). The aim of the non-crossing registration is to record the widest volume in which surgical manoeuvrability is maximal, as each point on the deep surface can be reached by all points in the superficial area. The aim of the crossing modality is to record the widest possible deep area; its periphery is made up of points that can be reached only through contralateral points on the superficial area (i.e. for bimanual surgery, the surgeon has to have an angled instrument in one hand to control that point with two instruments)

deep and superficial surfaces (i.e. at 3 o’clock at the pyriform aperture and at 9 o’clock at the posterior wall of the sphenoid sinus), defining the largest deep surface that can be reached with a straight instrument (Fig. 1).

ApproachViewer also allows a postdissection analysis to be performed by drawing areas of interest on the specimen CT scans [11, 12]. The drawings were done by tracing lines

extending from one side to the other side of the desired surface in each consecutive axial CT slice, which were automatically assembled to generate the surface. The following five areas were traced for this study: the lower clivus, the C0–C1 space, the anterior arch of the C1 vertebra, the odontoid process and the body of the C2 vertebra (Fig 2). The lower clivus area was defined by the floor of the sphenoid sinus as the superior border, by the lower end of the clivus as the inferior border and by the vertical projections of both hypoglossal canals as the lateral borders. The C0–C1 space area was the surface between the lower clivus and the anterior arch of C1, bound laterally by the occipital condyles. The anterior arch of the C1 vertebra was drawn from the upper border of the arch down to its lower edge, the lateral border being the junction between the arch and transverse processes. The odontoid process area corresponded to the space located between the anterior arch of C1 superiorly, the base of the odontoid process inferiorly and the medial border of C1–C2 articulation laterally. The body of the C2 vertebra area was defined as the anterior surface of the body of C2; its superior border corresponded to the base of the odontoid process, its inferior border was the inferior edge of the vertebra itself, and the lateral borders consisted of the lateral edges of the vertebra inferiorly and the junctions between the body and transverse processes superiorly (Fig. 2). Matching the areas of interest and the surgical pyramids, ApproachViewer provided absolute and percentage values of the surface exposed by each approach.

The height of each approach was calculated by measuring the distance between the midpoint of the superficial surface of the pyramid and the closest point on the odontoid process.

### **Radiological and Surgical Lines for the Endonasal Approach to the Craniovertebral Junction**

The nasopalatine line (NPL) [14] and the nasoaxial line (NAXL) [15] were drawn on CT scans (Fig. 3). The distance between the projections of the NAXL and NPL on the odontoid process was divided into five segments (Fig. 3). Subsequently, the segment reached by the most caudal point of the endonasal approaches was identified and recorded (Fig. 3).

### **Statistical Analyses**

Statistical analyses comparing the percentages of exposure provided by the endonasal and transoral approaches were



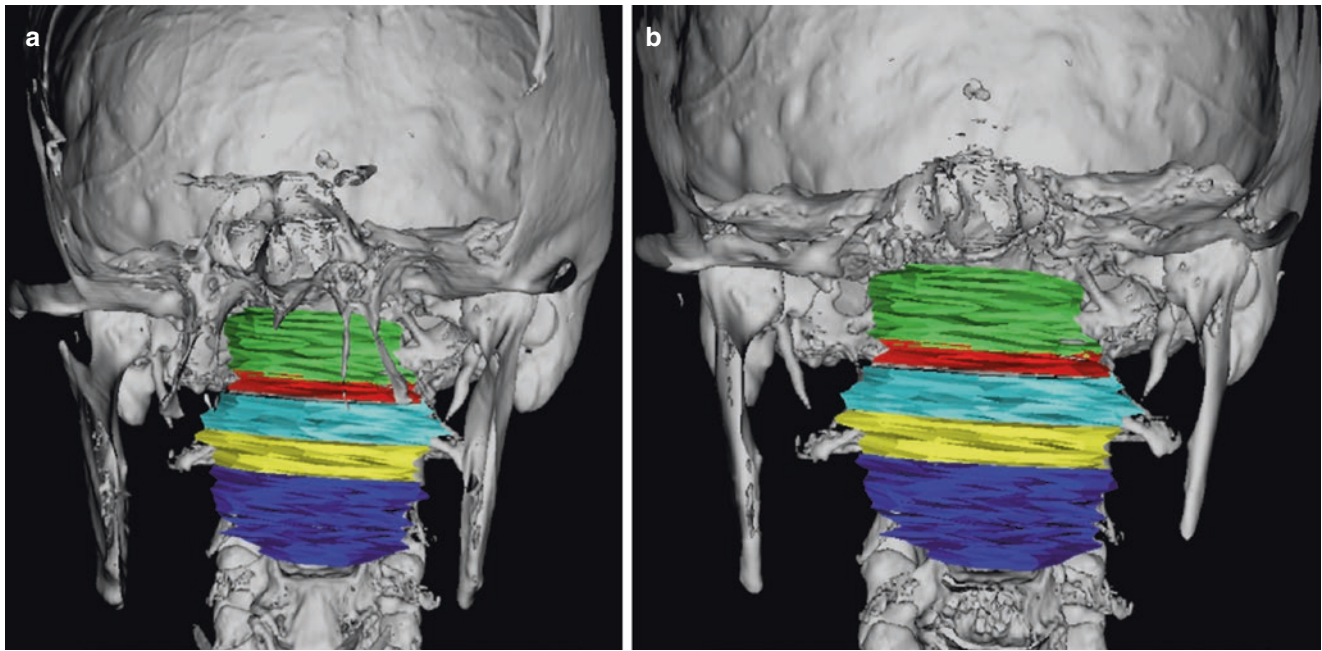


**Fig. 2** Anterior craniovertebral junction (CVJ) segmentation. In ApproachViewer, five different areas are drawn: the lower clivus (green), the C0–C1 space (red), the anterior arch of C1 (light blue), the

‘odontoid process’ (yellow) and the body of C2 (dark blue) (see text for further details). The same areas are shown with part of the sphenoid and pterygoid processes still visible (a) or removed (b)

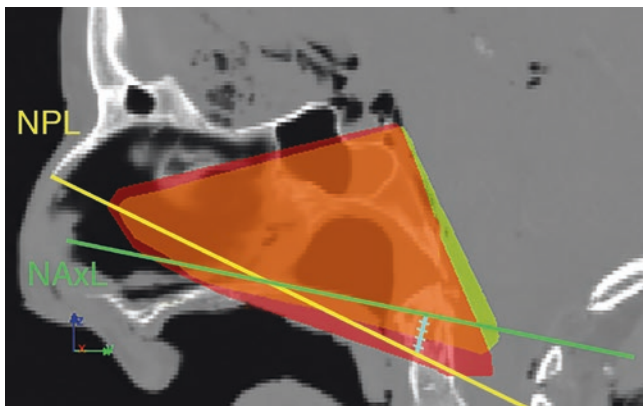


**Fig. 3** Predictive lines for endonasal approaches. The nasopalatine line (NPL; yellow) and the nasoxial line (NAXL; green) are drawn on computed tomography (CT) images on the midsagittal plane. The NPL is defined by the line that connects the inferior margin of the nasal bones anteriorly and the posterior border of the hard palate posteriorly [14]. The NAXL is the line that starts from the midpoint of the distance from the rhinion to the anterior nasal spine of the maxillary bone and ends at the C2 vertebra, tangential to the posterior nasal spine of the palatine bone [15]. The distance between the two lines at the level of the anterior craniovertebral junction (CVJ) is divided into five segments (blue line). The lowest point at the level of the anterior CVJ included in the non-crossing (yellow) and crossing (red) endonasal approaches is recorded (see text for further details)

performed for each area of interest. The same analyses were performed also for the heights and volumes of the approaches, but the crossing volumes were excluded, as they do not define a real working space.

The predictivity of the NAXL and NPL was analysed by recording where the lowest point of the surgical pyramids was for all endonasal approaches; crossing and non-crossing approaches were compared.

The normality and homogeneity of the variances were tested and demonstrated to not be present for each group of results. Therefore, non-parametric Welch analyses of variance (ANOVAs) were performed.

## Results

The mean operative volume of the endonasal approaches was 27.4 cm<sup>3</sup> before the sphenoidectomy, which led to a statistically significant increase to 53.3 cm<sup>3</sup> ( $p = 0.00005$ ) (Table 1). This gain of volume was directed superiorly, as shown in Fig. 3, and not relevant to surgical exposure of the odontoid process.

The mean operative volumes of the transoral approaches, without and with a soft palate split, were 82.2 and 111.5 cm<sup>3</sup>, respectively (with a gain of 26.37%); the difference between the two was not statistically significant (Table 1).

The approach height was significantly greater with the endonasal approaches than with the transoral approaches, with mean distances of 90.2 and 80.4 mm, respectively ( $p = 0.008$ ) (Table 1).

The analyses of the anterior craniovertebral areas exposed by each approach are summarized in Table 2. The lower

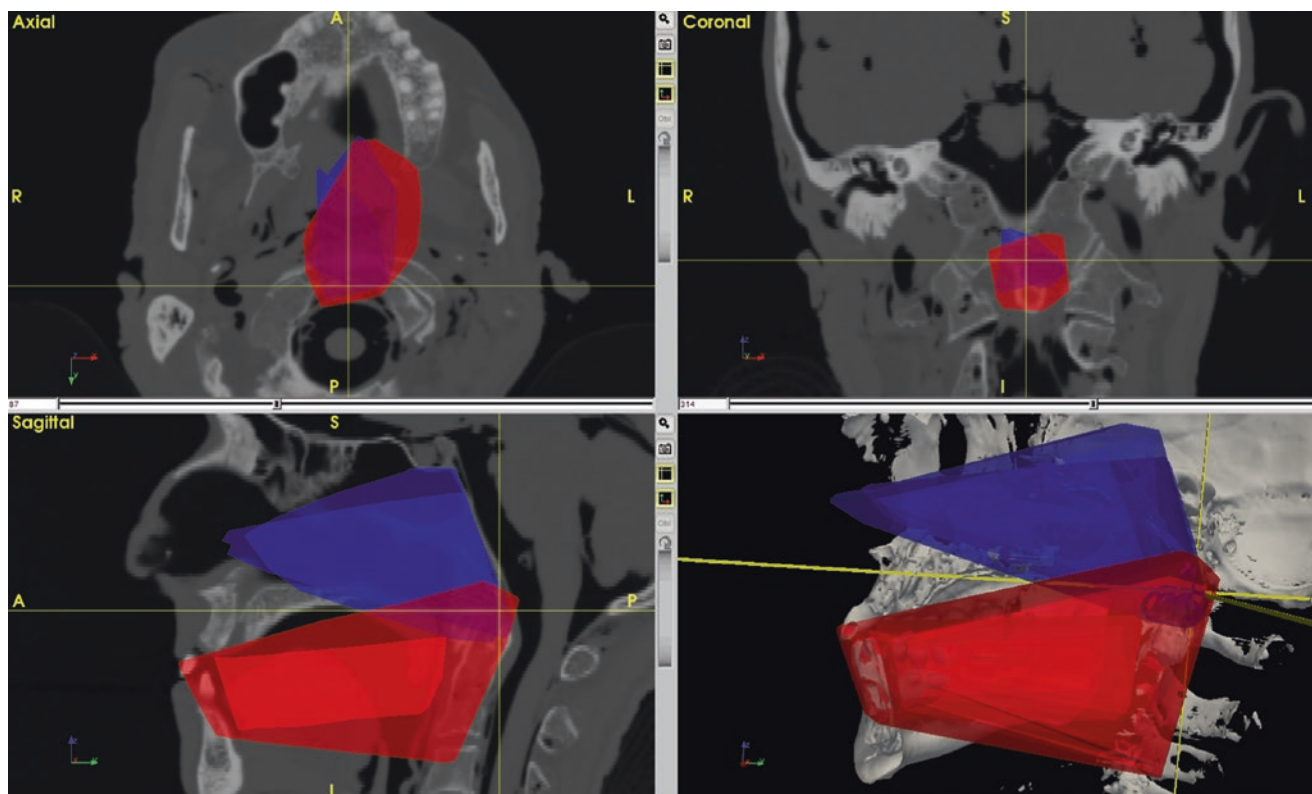


**Fig. 4** Areas shared by the endonasal and transoral approaches. The endonasal and transoral approaches share a common area at the level of C1, as shown on the three axes and with the reconstructed surgical volumes in ApproachViewer. An endonasal approach after sphenoidectomy

is shown in blue (lighter blue and larger volume: crossing; darker blue and smaller volume: non-crossing). A transoral approach without a soft palate split is shown in red (lighter red and larger volume: crossing; darker red and smaller volume: non-crossing)

**Table 1** Heights and volumes of transnasal and transoral approaches (see text for further details)

	Transnasal approach		Transoral approach	
Height [mm (range)]	90.22 (79.4–103.57)		80.35 (63.73–96.91)	
Volume [cm <sup>3</sup> (range)]	Without sphenoidectomy 27.42 (14.96–37.43)	After sphenoidectomy 53.30 (34.36–69.92)	Without soft palate split 82.16 (42.7–133.85)	After soft palate split 111.47 (57.68–147.5)

clivus exposures obtained with the crossing and non-crossing endonasal approaches (47.67% and 38.02%, respectively) were significantly larger than those obtained with the non-crossing transoral approach without a soft palate split (5.93%;  $p < 0.00001$ ).

The only statistically significant difference in C0–C1 surface exposure was between the crossing and non-crossing endonasal approaches (76.71% versus 55.91%;  $p = 0.01$ ).

A similar result was demonstrated for the C1 surface (62.38% versus 22.90%). The non-crossing endonasal approaches showed also significantly less exposure of the C1 surface than the crossing transoral approaches without a soft palate split (80.33%) and with a soft palate split (87.32%). The crossing transoral approaches with a soft palate split provided more exposure than the crossing endonasal approaches ( $p < 0.00001$ ).

The odontoid process surface (i.e. between the inferior margin of C1 and the body of C2; see Fig. 1) was significantly less exposed by the non-crossing and crossing endonasal approaches (0% and 10.54%, respectively) than by the non-crossing and crossing transoral approaches without a soft palate split (65.42% and 83.67%, respectively) and with a soft palate split (78.61% and 90.48%, respectively;  $p < 0.00001$  for the comparison between the endonasal and transoral approaches). Similarly, the C2 surface was more exposed by the transoral approaches than by the endonasal approaches ( $p < 0.00001$ ) (Table 1).

The Welch ANOVA performed on the segments reached by crossing versus non-crossing approaches showed that the mean segment reached by non-crossing approaches was the first (mean value 1.19) and the segment reached by crossing approaches was the third (mean value 2.89;  $p = 0.01$ ).

**Table 2** Percentages of the different areas of interest exposed by each approach (see text for further details)

	Value [% (range)]					
	TN	TN X	TO	TO X	TO-S	TO-S X
Lower clivus	38.02 (3.63–74.66)	47.67 (20.48–81.45)	5.93 (0–20.58)	35.53 (2.31–69.27)	22.23 (0–49.85)	55.77 (0–94.86)
C0–C1	55.91 (34.57–69.41)	76.71 (51.26–99.32)	29.52 (0–72.37)	69.86 (23.85–96.84)	57.32 (0–85.61)	72.44 (25.95–99.32)
C1	22.90 (0–51.61)	62.38 (43.69–83.01)	53.35 (0–80.88)	80.33 (51.6–96.71)	63.01 (17.42–79.62)	87.32 (77.14–94.3)
Odontoid	0 (0–0)	10.54 (0–45.61)	65.42 (0.91–88.32)	83.67 (64.68–100)	78.61 (70.61–94.86)	90.48 (76.22–100)
C2	0 (0–0)	0 (0–0)	35.09 (0.47–78.4)	71.71 (16.64–99.54)	51.79 (20.34–80.37)	86.26 (51.95–99.74)

TN transnasal, TN X transnasal, crossing, TO transoral, TO X transoral, crossing, TO-S transoral after soft palate split, TO-S X transoral after soft palate split, crossing

## Discussion

As the endonasal endoscopic approach to the CVJ has recently been added to the surgical armamentarium and the pathologies for which it is indicated are rare, clinical data are relatively scarce, as documented by a recent systematic review and meta-analysis that attempted a comparative analysis between transoral and endonasal approaches and was able to include only 92 patients who had undergone transnasal odontoidectomy [10].

Some authors have performed an anatomical comparative analysis of transoral and endonasal approaches to the anterior CVJ.

In this study we applied a new research method, based on the software ApproachViewer (part of GTx-UHN), which allows visualization and quantification of the surgical pyramid that defines an approach, as well as the absolute and percentage values of exposed areas of interest. The volumetric analysis confirmed what seems obvious to the experienced surgeon and has been qualitatively or indirectly demonstrated by others: the endonasal approach provides a significantly smaller working volume than the transoral approach. The height of the surgical pyramid proved to be significantly greater with the endonasal approach. These data are novel and do not confirm previous radiological analyses [16]. Together, these data describe what is qualitatively evident in the volume visualization: the endonasal approach is a significantly narrower corridor to the odontoid; it can be significantly augmented by sphenoidectomy, which provides a further cranial working volume (Fig. 4).

The exposed area analyses well documented that the endonasal approach provides less working space than the transoral approach: the crossing modality, which signifies the extreme surface touched by a straight instrument, almost always significantly led to an increase in exposure when compared with the non-crossing modality in the endonasal

approach. These data, though, were documented for each nasal cavity: in a standard odontoidectomy, a bi-nostril technique is used; furthermore, angled instruments might be used to augment the working space.

The comparative area analysis proved that there is a significant overlap between the endonasal and transoral approaches, as reported by others [8, 16–18]. In this study, the area was at the level of the anterior arch of C1. In a previous study of fresh cadavers with the aid of x-rays and CT scans, Visocchi et al. described the different angles that defined both approaches, and they defined the inferior third of the clivus as the shared surgical domain area [8]. The slight difference in these studies' data was most probably due to the difference in the specimens that were used.

As for the preoperative lines that predict the most inferior point exposed by the endonasal approach, we defined both the nasopalatine line (NPL, or 'Kassam' line) [14] and the nasoaxial line (NAXL) [15]. Our findings confirmed that the nasoaxial line best predicts the lowest point of the 'straight' working volume, i.e. the one with the greatest possible surgical manoeuvrability. The NPL was instead closer to the lowest possible point, exposed only by the crossing modality, i.e. the lowest point reached with an endonasal approach with a straight instrument. The inferior margin of the endonasal approaches, as measured by us and defined by the preoperative lines, does not take into account the possibility of using curved drills and instrumentation, which have already been developed for use in endonasal odontoidectomy; furthermore, we did not drill the posterior portion of the hard palate, which is another well-known procedure that can reduce the exposure obtained with an endonasal approach.

Though all of these data might seem obvious to the surgeon who is experienced in both approaches, they validate some clinical impressions and have clinical implications: (1) the transoral approach might be easier to perform because of the single and wider working space, but it will not effectively expose the clivus in most cases without a



soft palate split; (2) the endonasal approach requires specific training and angled instruments to fully take advantage of a narrower surgical corridor; and (3) a combination of these approaches eliminates the need for a soft palate split in the case of a transoral approach.

### Limits of the Present Study

The use of lightly embalmed rather than fresh specimens probably led to underestimation of both endonasal and transoral approaches due to relatively greater stiffness of the tissues.

We did not compare use of a microscope and an endoscope in the transoral approach. The aim of the study was to document the working volume of each approach, which is not influenced by the visualizing tool: as shown by the group led by Ammirati in an anatomical study [19] and by others in clinical reports [17, 20, 21], use of an endoscope can certainly increase visualization, but specific angled instrumentation might be needed to fully take advantage of endoscopic visualization and to optimize surgical manoeuvrability.

### Conclusion

The endoscopic endonasal and transoral approaches to the anterior craniovertebral junction provide optimal exposure of different areas that overlap at the level of C1 when no anatomical anomalies are present. A split of the soft palate is not necessary during a transoral approach if it is combined with an endoscopic endonasal approach. Detailed knowledge of the non-crossing volume that defines an approach might contribute to the development of optimal angled instrumentation.

**Acknowledgements** The authors would like to thank Lisa Satterthwaite and her team at the University of Toronto Surgical Skills Centre at Mount Sinai Hospital for their invaluable support during the anatomical dissections.

**Compliance with Ethical Standards** The study was approved by University of Toronto Research Ethics Board. Francesco Doglietto was in part sponsored by a grant from the Fondazione Giuseppe Alazio, via Torquato Tasso, 22, 90144 Palermo, Italy ([www.fondazionealazio.org](http://www.fondazionealazio.org)).

**Competing Interests** The authors declare that they have no competing interests.

### References

1. Alfieri A, Jho HD, Tschabitscher M. Endoscopic endonasal approach to the ventral cranio-cervical junction: anatomical study. *Acta Neurochir (Wien)*. 2002;144:219–25.
2. Cavallo LM, Cappabianca P, Messina A, Esposito F, Stella L, de Divitiis E, et al. The extended endoscopic endonasal approach to the clivus and cranio-vertebral junction: anatomical study. *Childs Nerv Syst*. 2007;23:665–71.
3. Kassam AB, Snyderman C, Gardner P, Carrau R, Spiro R. The expanded endonasal approach: a fully endoscopic transnasal approach and resection of the odontoid process: technical case report. *Neurosurgery*. 2005;57:E213.
4. Messina A, Bruno MC, Decq P, Coste A, Cavallo LM, de Divitiis E, et al. Pure endoscopic endonasal odontoidectomy: anatomical study. *Neurosurg Rev*. 2007;30:189–94.
5. Visocchi M. Transnasal and transoral approach to the clivus and the craniovertebral junction. *J Neurosurg Sci*. Epub 2015 Mar 4.
6. Visocchi M, Barbagallo G, Pascali VL, Mattogno P, Signorelli F, Iacopino G, et al. Craniovertebral junction transnasal and transoral approaches: reconstruct the surgical pathways with soft or hard tissue endoscopic lines? This is the question. *Acta Neurochir Suppl*. 2017;124:117–21.
7. Visocchi M, Germano A, Umana G, Richiello A, Raudino G, Eldella AM, et al. Direct and oblique approaches to the craniovertebral junction: nuances of microsurgical and endoscope-assisted techniques along with a review of the literature. *Acta Neurochir Suppl*. 2017;124:107–16.
8. Visocchi M, La Rocca G, Della Pepa GM, Stigliano E, Costantini A, Di Nardo F, et al. Anterior video-assisted approach to the craniovertebral junction: transnasal or transoral? A cadaver study. *Acta Neurochir (Wien)*. 2014;156:285–92.
9. Visocchi M, Pappalardo G, Pileggi M, Signorelli F, Paludetti G, La Rocca G. Experimental endoscopic angular domains of transnasal and transoral routes to the craniovertebral junction: light and shade. *Spine (Phila Pa 1976)*. 2016;41:669–77.
10. Shriver MF, Kshettry VR, Sindwani R, Woodard T, Benzel EC, Recinos PF. Transoral and transnasal odontoidectomy complications: a systematic review and meta-analysis. *Clin Neurol Neurosurg*. 2016;148:121–9.
11. Doglietto F, Qiu J, Ravichandiran M, Radovanovic I, Belotti F, Agur A, et al. Quantification and comparison of neurosurgical approaches in the anatomy laboratory: a novel, neuronavigation-based, research method. *Neurosurg Rev*. 2016;39(3):357–68.
12. Doglietto F, Qiu J, Ravichandiran M, Radovanovic I, Belotti F, Agur A, Zadeh G, Fontanella MM, Kucharczyk W, Gentili F. Quantitative comparison of cranial approaches in the anatomy laboratory: a neuronavigation based research method. *World J Methodol*. 2017;7(4):139–47. <https://doi.org/10.5662/wjm.v7.i4.139>.
13. Andaluz N, Van Loveren HR, Keller JT, Zuccarello M. Anatomic and clinical study of the orbitopterional approach to anterior communicating artery aneurysms: in reply. *Neurosurgery*. 2004;52:1140–9.
14. de Almeida JR, Zanation AM, Snyderman CH, Carrau RL, Prevedello DM, Gardner PA, et al. Defining the nasopalatine line: the limit for endonasal surgery of the spine. *Laryngoscope*. 2009;119:239–44.
15. Aldana PR, Naseri I, La Corte E. The naso-axial line: a new method of accurately predicting the inferior limit of the endoscopic

- endonasal approach to the craniovertebral junction. *Neurosurgery*. 2012;71:ons308–14.
16. Baird CJ, Conway JE, Sciubba DM, Prevedello DM, Quinones-Hinojosa A, Kassam AB. Radiographic and anatomic basis of endoscopic anterior craniocervical decompression: a comparison of endonasal, transoral, and transcervical approaches. *Neurosurgery*. 2009;65:158–64.
17. El-Sayed IH, Wu JC, Ames CP, Balamurali G, Mummaneni PV. Combined transnasal and transoral endoscopic approaches to the craniovertebral junction. *J Craniovertebr Junction Spine*. 2010;1:44–8.
18. Seker A, Inoue K, Osawa S, Akakin A, Kilic T, Rhoton AL Jr. Comparison of endoscopic transnasal and transoral approaches to the craniovertebral junction. *World Neurosurg*. 2010;74:583–602.
19. Pillai P, Baig MN, Karas CS, Ammirati M. Endoscopic image-guided transoral approach to the craniovertebral junction: an anatomic study comparing surgical exposure and surgical freedom obtained with the endoscope and the operating microscope. *Neurosurgery*. 2009;64:437–44.
20. Visocchi M, Della Pepa GM, Doglietto F, Esposito G, La Rocca G, Massimi L. Video-assisted microsurgical transoral approach to the craniovertebral junction: personal experience in childhood. *Childs Nerv Syst*. 2011;27:825–31.
21. Visocchi M, Doglietto F, Della Pepa GM, Esposito G, La Rocca G, Di Rocco C, et al. Endoscope-assisted microsurgical transoral approach to the anterior craniovertebral junction compressive pathologies. *Eur Spine J*. 2011;20:1518–25.